HHS Public Access

Author manuscript

Mol Neurobiol. Author manuscript; available in PMC 2018 August 01.

Published in final edited form as:

Mol Neurobiol. 2017 August ; 54(6): 4507–4523. doi:10.1007/s12035-016-9961-8.

Idiopathic autism: Cellular and molecular phenotypes in pluripotent stem cell derived-neurons

Xiaozhuo Liu[1,4,7], **Emilie Campanac**[2,7], **Hoi-Hung Cheung**[1,4], **Mark N. Ziats**[1,5,6], **Lucile Canterel-Thouennon**[1], **Margarita Raygada**[1], **Vanessa Baxendale**[1], **Alan Lap-Yin Pang**[1], **Lu Yang**[1], **Susan Swedo**[3], **Audrey Thurm**[3], **Tin-Lap Lee**[4], **Kwok-Pui Fung**[4], **Wai-Yee Chan**[4], **Dax Hoffman**[2,*], and **Owen M. Rennert**[1,*]

[1]Laboratory of Clinical and Developmental Genomics, National Institute of Child Health and Human Development (NICHD), National Institutes of Health (NIH), Bethesda, MD 20892, USA

[2]Molecular Neurophysiology and Biophysics Section, Program in Development Neuroscience, NICHD, NIH, Bethesda, MD 20892, USA

[3]Pediatrics and Developmental Neuroscience Branch, National Institute of Mental Health (NIMH), NIH, Bethesda, MD 20892, USA

[4]School of Biomedical Sciences, Faculty of Medicine, the Chinese University of Hong Kong, HK

[5]University of Cambridge, Cambridge CB3 9AN, UK

[6]Baylor College of Medicine, Houston, TX 77030, USA

Abstract

Autism spectrum disorder is a complex neurodevelopmental disorder whose pathophysiology remains elusive as a consequence of the unavailability for study of patient brain neurons; this deficit may potentially be circumvented by neural differentiation of induced pluripotent stem cells. Rare syndromes with single gene mutations and autistic symptoms have significantly advanced the molecular and cellular understanding of autism spectrum disorders, however, in aggregate they only represent a fraction of all cases of autism. In an effort to define the cellular and molecular phenotypes in human neurons of non-syndromic autism we generated induced pluripotent stem cells (iPSCs) from three male autism spectrum disorder patients who had no identifiable clinical syndromes, and their unaffected male siblings and subsequently differentiated these patient-specific stem cells into electrophysiologically active neurons. iPSC-derived neurons from these autistic patients displayed decreases in the frequency and kinetics of spontaneous excitatory postsynaptic currents relative to controls, as well as significant decreases in Na^+ and inactivating K^+ voltage-gated currents. Moreover, whole-genome microarray analysis of gene expression

*Correspondence: Dax Hoffman: hoffmand@mail.nih.gov, Address: Porter Neuroscience Research Center, Building 35, Room 3C-905, 35 Convent Drive, MSC 4995, Bethesda, MD 20892-4995. Owen M. Rennert, rennerto@mail.nih.gov, Address: 10 Center Drive, MSC 1255, Building 10, Room 1C-250, Bethesda, MD 20892-1255.

[7]Co-first author

Competing financial interests

The authors declare no competing financial interests.

Supplementary material

Supplementary material includes ten figures, four tables, and Supplementary methods.

identified 161 unique genes that were significantly differentially expressed in autistic patients iPSCs-derived neurons (> two-fold, FDR < 0·05). These genes were significantly enriched for processes related to synaptic transmission, such as neuroactive ligand-receptor signaling and extracellular matrix interactions, and were enriched for genes previously associated with autism spectrum disorder. Our data demonstrate aberrant voltage-gated currents and underlying molecular changes related to synaptic function in iPSCs-derived neurons from individuals with idiopathic autism as compared to unaffected siblings controls.

Keywords

Autism spectrum disorder (ASD); induced pluripotent stem cell (iPSC); iPSC-derived neuron; synaptic transmission; gene expression

Introduction

Autism spectrum disorder (ASD) is a heterogeneous group of disorders with a prevalence of one in 60 to 70 children [1]. This grouping of ASD is characterized by core symptoms of behavioral deficits and extended phenotypes (associated clinical features). The core symptoms, which vary in severity, include persistent behavioral deficits in social interaction and communication, repetitive behaviors, and restricted social interests. Autism is called a "spectrum disorder" because of the extraordinary heterogeneity of the severity of core symptoms, the extended phenotypes, and possible their divergent etiology [2]. Extended ASD phenotypes include seizures, intellectual disability, speech and other developmental delays, dysmorphic features, cardiac arrhythmias, skin manifestations, hematoma, comorbidity diseases, male preponderance, gene associations and other manifestations. ASD is comorbid with a number of other diseases, including tuberous sclerosis, Fragile X syndrome, Timothy syndrome, male Rett syndrome (with *MECP2* gene mutation), and chromosomal abnormalities syndromes (Angelman, Prader-Willi, Phelan-McDermid and other syndromes). ASD is skewed towards boys, with a sex ratio of at least 2·7 to 1 [3]. Large population genome-wide association studies (GWAS) [4], *de novo* mutations [5] and copy number variation (CNV) [6] studies have identified hundreds of genes and genomic regions significantly associated with ASD [7]. To date, more than 500 genes and 44 genomic loci have been associated with the symptom/syndrome complex of ASD [8]. Though there is a strong genetic basis for ASD, the majority of cases have unknown causes. Identifiable single gene disorders such as tuberous sclerosis have been identified in 10% of ASD individuals; known chromosomal abnormalities such as 22q13·3 deletion have been identified in 5–10% of cases [9]. However, none of these etiologies alone account for more than 2% of cases [7].

The common feature of all these syndromes, together with extended phenotypes, is dysfunctional socialization and communication, and stereotyped and repetitive behavior. Brain imaging studies have failed to identify consistent anatomic abnormalities that are unique to "autism" though they are useful diagnostic adjuncts. The unifying feature that has emerged from functional magnetic resonance imaging is that the brain exhibits "altered connectivity, specifically increased local short-distance connectivity, and decreased long-

distant connectivity" [10, 11]. A central hypothesis that has been proposed is altered synaptic transmission [12]. However, the paucity of patient brain tissue, and genetic heterogeneity make it difficult to explore the molecular and cellular pathophysiology of ASD. This deficit may be circumvented through the use of neural differentiation of induced pluripotent stem cells (iPSCs) [13]. Patient-specific iPSCs maintain the genetic background of parental cells, a feature critically important for the study of disorders with complex genetics such as ASD [14]. *Our postulation is that multiple genetic mutations give rise to dysfunctional transcription and/or translation which, at different times in brain development, or in different regions of the brain give rise to the socialization and communication deficits that are part of multiple syndromes accounting for ASD. We also postulate that iPSC-derived neurons from ASD individuals will exhibit altered synaptic transmission (cultured cell phenotype), and that altered gene expression will mimic or reflect many of the gene-associations that have been characterized from genetic studies of ASD.*

In this small preliminary study, we studied a relatively clinically homogeneous patient population with idiopathic forms of ASD, and distinguished them from patients with known genetic disease or a recognizable syndrome. We excluded patients with severe intellectual disability, primary seizure disorders, or known syndromes or malformations. In addition, relative homogeneity of these patients was also based on all male sex, age ranges (5 – 16 years), no dysmorphic findings, nor other neurologic deficits. We also studied unaffected male siblings of these patients as controls. We derived iPSCs from skin-fibroblasts from ASD patients and their unaffected male siblings, differentiated them into mature cortical-like neurons. Comparison of autistic patient and control iPSC-derived neurons by morphological (synaptic density), electrophysiological (whole-cell patch clamp recordings) and transcriptional analyses (global transcriptome analysis) showed aberrant cellular and molecular phenotypes in synaptic transmission and voltage-gated ion channels. Substantially greater numbers of patient-specific iPSC-derived neuron must be generated in future investigation of larger cohorts to validate this preliminary study.

Materials and methods

Additional details are provided in the Supplementary material section.

Experimental design

We studied a clinically homogeneous cohort of male patients with idiopathic forms of ASD and did not have severe intellectual disability, primary seizure disorders, or known syndromes or malformations (Fig. 1A). Skin fibroblasts were obtained from three male patients with ASD and their unaffected neurologically-normal age-matched male siblings, as well as two age- and sex-matched unrelated healthy donors. Characteristics of patients and sib controls are described in Table 1 and Supplementary Table 1. We first optimized protocols including iPSCs generation from skin fibroblasts (Supplementary Fig. 1A) and neural differentiation from iPSCs (Supplementary Fig. 5A and Fig. 2A). We performed extensive quality control analyses (pluripotency characterization, karyotyping) to select iPSC lines from each donor, differentiated iPSC lines into mature cortical-like neurons, which fired action potentials and formed functional synapses. Through comparison of

autistic patient and control iPSC-derived neurons, we investigated the cellular phenotypes of ASD *in vitro* from three aspects: morphological (synaptic density), electrophysiological (whole-cell patch clamp recordings) and transcriptional analyses (global transcriptome analysis) (Fig. 1A).

Recruitment of patients with idiopathic form of ASD

Participants with idiopathic forms of ASD were recruited from ongoing research studies in the NIH Clinical Center Genetic Clinic. Additionally, the unaffected, neurologically-normal age- and sex-matched siblings of these patients, as well as age- and sex-matched unrelated healthy donors were also recruited as controls. All participants or their legal guardian gave informed written consent. Consenting participants were evaluated with the Autism Diagnostic Observation Schedule-Generic (ADOS-G) [15] and clinical assessment. In addition, parents of participants completed the Autism Diagnostic Interview-Revised (ADI-R) [16] and questionnaires about the participants, including a medical history. Genetic evaluation was performed by a geneticist and genetic counselor including physical examination, molecular diagnostic tests, and comparative genomic hybridization analysis. All participants also received cognitive testing and a parent-administered interview regarding adaptive behavioral functioning, and several other neuropsychological instruments under the NIMH screening protocol #06-M-0065. Patients were included in this study only if they did not have an identifiable clinical syndrome, had a normal karyotype, and did not have identifiable pathogenic mutations on comparative genomic hybridization testing. We also excluded patients with severe intellectual disability or primary seizure disorders (see Table 1 patient information). This study was approved by NICHD Institutional Review Board (IRB number 10-CH-0084).

Skin biopsy procedure and skin-fibroblast culture

Participants underwent a punch biopsy of the forearm skin using standard procedures. Briefly, after local anesthesia with 1% xylocaine, a shallow, 3–6 mm biopsy was obtained from the mesial aspect of the forearm. Human skin fibroblasts were maintained in MEM (Corning) supplemented with 15% (vol/vol) non-heat inactivated Fetal Bovine Serum (FBS) (American Type Culture Collection, ATCC), 1% non-essential amino acids (NEAA) (Corning), and 1% antibiotics (Corning).

Cell lines and cultures

hESC lines CT2 and ESI-053 were obtained from University of Connecticut Stem Cell Core and BioTime, respectively. All cell cultures were maintained as suggested by the providers. Human embryonic kidney cells 293FT cells (Life Technologies) were maintained in Dulbecco's modified Eagle's medium (DMEM) (Life Technologies) supplemented with 10% heat inactivated-FBS (Life Technologies), 1% NEAA, and 1% antibiotics. Irradiated CF1 mouse embryonic fibroblasts (MEFs) were from Applied StemCell and incubated in MEF medium: DMEM with 10% heat inactivated-FBS, 1% GlutaMAX (Life Technologies), and 1% antibiotics.

Generation and characterization of iPSC

Generation, maintenance, and characterizations of iPSCs were performed as described elsewhere [17], with specific modifications described in the Supplementary material. iPSCs and hESC were cultured on MEF feeders in iPSC medium (Knockout DMEM (Life Technologies), containing 20% Knockout SR (Life Technologies), 1% GlutaMAX, 0.1 mM β-mercaptoethanol (Life Technologies), 1% antibiotics, 1% NEAA, and 10 ng/ml basic fibroblast growth factor (bFGF) (Peprotech). For characterization procedures of iPSCs, see Supplementary material.

Neural induction and differentiation from iPSCs

Neural induction—Neural progenitor cells (NPCs) differentiation from iPSCs was induced through embryoid bodies (EBs) formation as described by Marchetto *et al* [18]. with slight modifications described in the Supplementary material.

Post-mitotic neural differentiation—To further differentiate into post-mitotic neurons, NPCs were plated onto Poly-D-lysine (PDL) (Sigma) and laminin (Sigma) double-coated German glass coverslips (Neuvitro) (10000 cells per cm^2) overnight in NPC media [0·5% N2 (Life Technologies), 1% B27 (without Retinoic acid) (Life Technologies), 1% GlutaMAX, 1% NEAA, EGF (20 ng/ml) (Peprotech), and bFGF (20 ng/ml) in DMEM/F12 medium (Life Technologies)]. On day 2, neural differentiation was induced by withdrawing EGF and bFGF and switching to neural differentiation medium consisting 1% N2, 2% B27 (without Retinoic acid), 1% GlutaMAX, 1% antibiotics, BDNF (10 ng/ml), GDNF (10 ng/ml), IGF-1 (10 ng/ml), and cyclic adenosine monophosphate (cAMP) (1μM, Sigma) in Neurobasal medium (Life Technologies) (All neurotrophic factors were from Peprotech). Cells were fed every other day by removing one-half the volume of medium and replacing the medium with fresh warmed medium pre-equilibrated with 95% O_2 and 5% CO_2 at 37°C. iPSC-derived neurons were differentiated for 2–3 months. For characterization procedures of neural rosettes, NPCs and post-mitotic neurons, see Supplementary material.

Immunofluorescent staining and confocal microscopy

Cells were grown on glass cover slides. Following washing with ice-cold phosphate buffered saline (PBS), the cells were fixed in 4% paraformaldehyde (w/v) in PBS at 4°C for 10 minutes. Cells were then permeabilized at room temperature for 15 minutes in 0·1% Triton in PBS. Cells were blocked in 5% goat or donkey serum with 0·1% Triton at room temperature for 30 minutes. Cells were incubated with primary antibodies for overnight at 4°C, followed by 30 minutes to 1 hour incubation with species-specific Alexa-dye conjugates secondary antibodies from Life Technologies. Primary and secondary antibodies, and their working dilutions were described in the Supplementary material. The cells were thoroughly washed with PBS and examined by a Zeiss Axiovert-200 fluorescence microscope and Images were acquired using AxioVision 3·8 software (Carl Zeiss). For confocal analysis, the samples were examined with a Zeiss LSM 510 confocal microscope.

Neurite analysis, synaptic-associated marker expression and flow cytometry

See Supplementary material for description of procedure.

Electrophysiology

Whole cell patch clamp recordings were obtained from iPSC-derived neurons at 8–12 weeks after neuronal differentiation induction. For detailed description of current clamp, voltage clamp, solutions, drugs, data acquisition, analysis and statistics, see Supplementary material.

Statistical analysis of cellular studies

For neuronal morphology and flow cytometry experiments, all comparisons between autistic patient and control samples were tested by unpaired, two-tailed Student's t-test. A *p-value* < 0·05 was considered significantly different.

For electrophysiology experiments, pooled data are presented as either mean ± SEM or box plots and statistical analyses were performed using Mann-Whitney U-test. *p* values are reported in the text or figures with values < 0.05 considered as significant (* $p<0{\cdot}05$).

RT-PCR, microarray analysis and bioinformatics analysis

Quantitative real-time RT-PCR—For detailed description of quantitative PCR, and primers used for PCR amplification of selected genes, see Supplementary material.

Microarray analysis—Whole-genome expression profiles were assessed with Affymetrix GeneChip® Human Gene 1·0 ST Array (Affymetrix). See Supplementary material for detailed description of microarray procedures. To analyze differentially expressed genes, we first removed batch effects and then compared the difference of the mean expression for each gene by student T-test. We clustered the iPSC-derived neurons samples based on the differentially expressed gene sets. Genes with fold change > 2 or < −2 and a false discovery rate (FDR) *p-value* < 0·05 were considered significant.

GO categories—To assess for functional categories that the genes we identified as significantly differentially expressed in ASD implicated, we used the Database for Annotation, Visualization and Integrated Discovery v6·7, accessed at http://david.abcc.ncifcrf.gov. GO categories were reported as significant only if the *p-value* after multiple testing corrections was <0·05.

Integrated gene-network analysis—Integrated gene-network analysis was generated using Ingenuity Pathways Analysis (Version 8·8, Ingenuity® Systems, www.ingenuity.com). See Supplementary material for procedures of analysis. Functional Network Analysis identified the biological interactions that were most significant to the molecules in the network. A *p-value* of less than 0·05 was considered significant. The network molecules associated with biological functions and/or diseases in Ingenuity's Knowledge Base were considered for the analysis. Right-tailed Fisher's exact test was used to calculate a *p-value* determining the probability that each biological function assigned to that network is due to chance alone, with a threshold of 0·05 set for significance.

Autworks Gene-Disorder Analysis—The overlap of the identified differentially expressed genes with other neurodevelopmental disorders was assessed using the Autworks

Gene-Disorder Analysis software, accessed at: http://autworks.hms.harvard.edu/. Default parameters were used throughout the analysis.

Accession number—Microarray data were deposited in the National Center for Biotechnology Information Gene Expression Omnibus database under the accession ID GSE65106.

Results

Patient recruitment and derivation of iPSC lines

Participants with idiopathic forms of ASD and their unaffected healthy siblings, as well as age- and sex-matched unrelated healthy donors were recruited from ongoing research studies in the NIH Clinical Center Genetic Clinic. As shown in Fig. 1A and Table 1, the autistic patients we studied in this small preliminary study, none of them have a recognizable syndrome associated with ASD (based on assessment by geneticists), have been shown by molecular studies not to have disorders such as Fragile X, Rett (atypical) syndrome, tuberous sclerosis, neurofibromatosis type 1 and other identifiable syndromes. These patients have had array studies (CGH) which were non-diagnostic, but have not had whole exome sequencing. Imaging studies (MRI) were non-diagnostic. In addition, relative homogeneity of these patients was based on all male sex, age ranges from 5 – 16 years, no dysmorphic findings, moderate intellectual disability, no history of seizures, nor other neurologic deficits (Table 1). Skin fibroblasts were obtained from three male patients with ASD and their unaffected male siblings. The participants AA1, AA2, and AA3 in this study met criteria for ASD based on the ADI-R [16] and the ADOS-G [15] assessment, and were given a diagnosis of ASD after an additional thorough clinical assessment by pediatrician and neurologist in NIH Clinical Center Genetic Clinic. Characteristics of patients and sib controls are described in Table 1.

To generate iPSC lines, patient and control fibroblasts were infected with polycistronic lentivirus expressing human OCT4, SOX2, KLF4 and c-MYC [19], as described elsewhere [17]. Round and flattened reprogrammed colonies emerged from a background of fibroblasts two weeks after infection (Supplementary Fig. 1). Reprogrammed colonies with similar morphology to human embryonic stem cells (hESCs) and positive for TRA-1–60 (a surface marker associated with pluripotency) immunostaining were initially selected and passaged manually (Supplementary Fig. 1), and subsequently validated using immunostaining to verify expression of pluripotency markers.

We performed extensive quality control analyses to select iPSC lines from each donor. Similar to hESC lines ESI-053 and CT-2, these selected patient-specific iPSC lines showed hESCs colony morphology, and positive expression of pluripotency markers NANOG, OCT4, SOX2 (in the nucleus) and surface markers SSEA4, TRA-1-60 and TRA-1-81 by immunostaining (Supplementary Fig. 2). All iPSC lines maintained a normal male karyotype throughout passaging (Supplementary Fig. 3A). Pluripotency of iPSC was examined by teratoma formation assay *in vivo*. Histological analysis of the teratoma sections revealed organized structures representing tissues from three germ layers, such as gland and duct structure from endoderm, bone and white adipocytes from mesoderm, and neural rosettes

and pigmented neural cells from ectoderm (Supplementary Fig. 3B). Additionally, Microarray analysis indicated iPSC global gene expression was similar to hESCs, but distinct from their parental fibroblast cells (Supplementary Fig. 4). Based on demonstration of normal karyotypes, pluripotent marker expression, capability to generate three germ layers *in vivo*, and global expression profiles similar to hESCs, iPSC lines were selected for neural differentiation, cellular and molecular characterization (Fig. 1B and see Supplementary Table 1 list of cell lines used).

Autistic patient iPSCs can be differentiated into functional and electrophysiological active neurons *in vitro*

We differentiated iPSCs into neural progenitors and neurons using conditions favoring generation of cortical neurons (Fig. 2A) [20–23]. Neural progenitor cells (NPCs) differentiated from iPSCs through embryoid body intermediates exhibited neural progenitor markers SOX1 and NESTIN (Supplementary Fig. 5). NPCs were differentiated into post-mitotic neurons by withdrawing growth factors bFGF and EGF. Cells were cultured in the presence of BDNF, GDNF, IGF, ascorbic acid and cAMP for more than 8 weeks to promote terminal differentiation (Fig. 2A and B).

Differentiated neurons expressed pan-neuronal markers TUJ-1 and MAP2 (Fig. 2C). In addition, we observed glial lineage cells, such as GFAP-positive astrocytes and A2B5-positive Type 2 astrocytes (Fig. 2C). There were approximately 82% MAP2-positive neuronal cells and 15% GFAP-positive glial cells in the culture (Fig. 2D). Further characterization of the neurons showed that the majority (~ 70%) of MAP2-positive neurons were Glutamate-positive glutamatergic neurons, and approximately 30% of the neurons were GABAergic neurons, while less than 5% were dopaminergic neurons (Fig. 2E).

iPSC-derived neurons following 80 days of post-mitotic neural differentiation expressed synaptic-associated proteins synaptophysin (SYN) along the dendritic arbors of neuron (Fig. 2F), indicating formation of synapse and maturation of neural culture. In agreement with morphological data, whole-cell patch clamp recordings showed that both autistic patient and control iPSC-derived neurons fired trains of action potentials in response to somatic current injection of 10 pA (Fig. 2H and Supplementary Fig. 6A). Both showed Na^+ and K^+ voltage-gated currents in response to a depolarizing voltage step (Fig. 2J and Supplementary Fig. 6B). Bath application of tetrodotoxin (TTX), a specific Na^+ voltage-gated channel blocker, suppressed action potentials (Fig. 2I) and Na^+ current (Fig. 2K). Thus, both autistic patient and control iPSC cells differentiated into electrophysiologically active neurons. These patient-specific neurons might allow identification of cellular phenotypes and examination of the molecular basis of the disease. We next investigated morphological (synaptic density), electrophysiological (whole-cell patch clamp recordings) and transcriptional differences of iPSC-derived neurons from autism as compared to their male sib controls (Fig. 1B).

Neurons derived from autistic patient iPSCs displayed altered spontaneous excitatory postsynaptic currents

We studied neurite outgrowth number and synaptic-associated protein density to investigate morphological phenotypes of iPSC-derived neurons. The number of neurites was unaltered

between autistic patient and control iPSC-derived neurons (Fig. 3A and B). Figure 3C illustrates cellular location of pre- and post-synaptic proteins in excitatory and inhibitory neurons. Both autistic patient and control iPSC-derived neurons expressed pre- and postsynaptic markers, including SYN, PSD-95, vesicular glutamate transporter 1 (VGLUT1), and vesicular GABA transporter (VGAT), indicative of neuronal maturation (Fig. 3D). Though synaptic-associated proteins densities of autistic patient and control iPSC-derived neurons were not significantly different, we observed slightly decreased densities of SYN, PSD-95, VGLUT1 and VGAT puncta in autistic patient iPSC-derived neurons (Fig. 3E).

Spontaneous inhibitory postsynaptic currents (sIPSCs) and excitatory postsynaptic currents (sEPSCs) were measured to assess intercellular connectivity and network formation [18]. Both sIPSC and sEPSC events were observed in autistic patient and control iPSC-derived neuronal cultures (Fig. 3F and G), indicating that iPSC-derived neurons formed functional synapses and integrated into neural circuits *in vitro*. sEPSC analyses revealed that sEPSC frequency and half width were significantly reduced in autistic patient iPSC-derived neurons whereas amplitude and rise-time remained unchanged (Fig. 3H), most likely indicating a presynaptic defect in synaptic release [24]. *These data suggest that neuronal network activity is altered in autistic patient iPSC-derived neuron cultures. These data indicate that iPSC-derived neurons show in vitro maturation of intrinsic excitability, laying the groundwork for a detailed comparison of intrinsic electrophysiological properties between ASD and controls.*

Autistic patient iPSC-derived neurons displayed altered excitability, aberrant Na^+ and fast K^+ voltage-gated currents

To examine intrinsic electrophysiological properties of iPSC-derived neurons, we first analyzed the I/V curve and the input resistance, but no significant differences were observed between autistic patient and control iPSC-derived neurons (Fig. 4A and B). Analysis of the firing phenotype of these neurons through the Input-Output function revealed that autistic patient iPSC-derived neurons reach action potential saturation significantly sooner as compared to controls (Fig. 4D, *p-value* = 0·0393). Finally, we measured parameters of the first action potential during a current ramp of 40 pA/s, including rheobase, threshold, maximum, amplitude, latency and half width (Fig. 4E–4G). Although these parameters were not significantly different in both groups, autistic patient iPSC-derived neurons showed a trend of more excitable stage as shown by the parameters of action potential number, rheobase, threshold and latency (Fig. 4C, F and G).

To confirm neuronal identity and maturity of the cells, we recorded main known neuronal voltage-gated currents: Na^+, K^+ and Ca^{2+}. All of these currents were present in autistic patient and control iPSC-derived neurons (Fig. 4H–4J). No differences were observed in either Ca^{2+} or slow inactivating K^+ (also known as D-type Kv) voltage-gated currents (Fig. 4H and J). *However, significant decreases in both Na^+ and fast inactivating K^+ (also known as A-type Kv) voltage-gated currents were observed in autistic patient iPSC-derived neurons (*Fig. 4H and I).

Differentially expressed genes in autistic patient iPSC-derived neurons revealed core pathways in synaptic transmission

Principal component analysis (PCA) for global gene expression of iPSC-derived neurons revealed that samples from autistic patients cluster together and are separate from their unaffected sib controls (Fig. 5A). We identified differentially expressed genes between iPSC-derived neurons from autistic patients as compared to their unaffected siblings (Fig. 5B). In total, 161 unique genes (109 up-regulated and 52 down-regulated) showed greater than two-fold-expression changes between autistic patient and control iPSC-derived neurons with a FDR less than 0·05 via microarray (Fig. 5B and Supplementary Table 2). We confirmed a subset of these genes via quantitative PCR (Supplementary Table 3). Twenty-two genes (14%) with altered expression in autistic patient iPSC-dervied neurons have previously implicated in ASD (Fig. 5C) and annotated in the SFARI Gene Database (https://gene.sfari.org), including many with strong association to ASD such as cadherin 10 (*CDH10*), neurexin 3 (*NRXN3*), synapsin III (*SYN3*), dipeptidyl peptidase 10 (*DPP10*), gamma-aminobutyric acid (GABA) A receptor alpha 3 (*GABRA3*) and voltage-gated Na^+ type II alpha subunit (*SCN2A*) (Fig. 5C). This enrichment for known ASD candidate genes was highly significant ($p\text{-value} = 2{\cdot}21\times10^{-9}$) (Fig. 5C). Additionally, gene ontology (GO) analysis of these 22 differentially expressed genes previously implicated in ASD revealed a number of significant pathways ($p\text{-value} < 0{\cdot}05$) related to synaptic function (synapse, postsynaptic membrane, synaptic transmission, synaptogenesis, and integrin signaling), neurotransmitter function (neurotransmitter receptor activity, neurotransmitter secretion/binding), and ion channels function (extracellular ligand-gated ion channel activity, GABA-A receptors activity) (Supplementary Table 4).

GO analysis of all 161 differentially expressed genes identified significant enrichment of processes related to nervous system development, transmission of nerve impulse as well as mechanisms of synapse formation such as GABAergic synapse pathway, PI3K-Akt signaling, neuroactive ligand-receptor interaction and extracellular matrix (ECM)-receptor interaction (Table 2). The 161 differentially expressed genes were analyzed for gene interaction networks using the Ingenuity Pathway Analysis (IPA) database. Several significant interaction networks were identified, with central nodes that support the GO enrichment results, such as ERK1/2, integrin, insulin, GABA receptors, Matrix metallopeptidase 9 (MMP9), cAMP responsive element binding protein (CREB), PI3K-Akt signaling and ubiquitin C (Table 3 and see Supplementary Fig. 7–9 for IPA network illustrations). Moreover, the predicted upstream fundamental regulators of these networks include canonical signaling molecules such as Catenin (Cadherin-Associated Protein) beta 1 (*CTNNB1*), GABA-A receptor alpha 1 (*GABRA1*), RE1-Silencing Transcription Factor (*REST*), and huntingtin (*HTT*) (Fig. 5D). Top-ranked gene interaction networks were enriched for the IPA terms “nervous system development and function,” “hereditary disorder,” “psychological disorders,” “neurological disease,” “nutritional disease,” “behavioral disorders,” “developmental disorder,” and “ophthalmic disease” (Table 3). These results raised our interest to explore the overlap of the differentially expressed genes in our autistic patient iPSC-derived neurons with genes previously implicated in other psychiatric disorders, as the genetics underlying various psychiatric disorders have been shown to be overlapping [25]. Gene-disorder association analysis from Autworks database (http://

autworks.hms.harvard.edu) [26] showed the 161 differentially expressed genes in autistic patient iPSC-derived neurons were significantly associated with childhood schizophrenia, epilepsy, neurotic disorders, and autistic disorder (*p-value* < 0·05) (Table 2). This is particularly intriguing given the significant co-morbidity of these disorders in autistic patients.

Discussion

As more and more evidence accumulated, it was well accepted that autistic behaviors resulted from dysregulated brain development [27], altered brain structure [28] and functional connectivity [10, 11, 29]; and "a disease of abnormalities in synaptic transmission of neurons" becomes the major hypothesis for the cellular basis of ASD [12]. Despite this hypothesis has gained indirect support from human post-mortem brain examination, animal models and genetic studies [12, 30, 31], little is known about the pathophysiology of live patient neurons. Using human iPSC-derived neurons to model brain networks has great potential to improve our understanding of human-specific neurodevelopmental disorders such as ASD. Here, we demonstrate that iPSC-derived functional neurons provide important insights of idiopathic forms of ASD at both the cellular and genomic levels. We identified 161 differentially expressed genes in autistic patient iPSC-derived neurons as compared to unaffected siblings, which were enriched for ion channels and synaptic functions. These results, together with cellular-level analysis demonstrating aberrant voltage-gated currents and globally altered neural networks in the autistic patient iPSC-neuron cultures, suggest the iPSC strategy can be effectively utilized to model idiopathic forms of ASD. Thus, iPSC-derived neurons from idiopathic forms of ASD patients appear to recapitulate the elements of the disorder contributed by complex genetic components, potentially serving as a valuable model for further investigation of idiopathic forms of ASD.

A number of previous studies have investigated syndromic or single-gene causes of ASD using iPSC-derived neurons. It has been documented that iPSC-derived neurons display cellular phenotypes such as abnormal synaptic transmission for ASDs with known gene mutations (*MECP2*, *CACNA1C*, *SHANK3*) [18, 32–34] or chromosomal abnormalities (15q11-q13, 22q13·3) [35–37] as well as for a non-syndromic ASD case with *de novo* balanced translocation disruption of *TRPC6* [38]. For instance, iPSC-derived neurons generated from children with Rett Syndrome have smaller soma size, fewer synapses, reduced spine density, altered calcium signaling, and electrophysiological defects [18] - cellular characteristics similar to those observed in post-mortem Rett Syndrome brains [39] and animal models [40]. iPSC-derived neurons from patients with *SHANK3* mutations, a rare but highly penetrant ASD-associated variant, were reported to have excitatory neuron dysfunction [36]. Moreover, a recent study using iPSC-derived neurons from a non-syndromic ASD case caused by *de novo* translocation of *TRPC6* demonstrated that Na^+ currents of *TRPC6*-mutated neurons were impaired as compared to controls [38]. Our iPSC-derived neurons from idiopathic forms of ASD patients replicate some of these findings from syndromic ASD. For example, the electrophysiological properties of these ASD patient iPSC-derived neural cultures showed significant decreases in the frequency of sEPSC relative to controls, suggesting a presynaptic impairment in synaptic transmission [24] and

that the global neuronal network is altered in autistic patient iPSC-derived neuron cultures [18].

In addition, our electrophysiological results also provide new observation on cellular phenotypes of ASD patient iPSC-derived neurons. Genetic studies have previously linked the role of ion channel genes defects in the pathogenesis of ASD like alternation of brain excitability [41–43]. However, little is known about the ion channel function of live patient neurons. Our electrophysiological results of ASD patient iPSC-derived neural cultures showed significant decreases in both Na^+ and fast K^+ voltage-gated currents, but not in Ca^{2+} and slow K^+ voltage-gated currents. The reduction of Na^+ and fast K^+ voltage-gated currents likely accounts for the observation that autistic patient iPSC-derived neurons have altered excitability since these two currents greatly impact action potential firing properties [42]. Meanwhile, our gene expression results of patient iPSC-derived neurons also suggested ion channel defects could be cellular phenotypes associated with ASD. We found that differentially expression of genes of sodium and potassium channels and their subunits in ASD patient iPSC-derived neurons, including voltage-regulated sodium channel type 2 *SCN2A* and potassium voltage-gated channel (A-channel) *KCND2*. Through applying neural morphological and electrophysiological analysis on live neurons derived from patient-specific iPSCs, we may gain alternative evidences to study pathogenesis of ASD, in addition to indirect support from human post-mortem brain examination, animal models and genetic studies.

In addition to recapitulating the cellular-level findings of previous studies of autistic patient iPSC-derived neurons, our results also demonstrated the iPSC-neurons from idiopathic forms of ASD patients retain gene expression signatures relevant to previously identified ASD candidate genes and molecular pathways. For instance, the differentially expressed genes in autistic patient iPSC-neurons compared to their unaffected siblings were significantly enriched for genes previously implicated in ASD, such as *CDH10*, *DPP10*, *GABAR3*, *NRXN3*, *SCN2A, and SYN3*. Defects of voltage-gated K^+ channels (Kv) have been correlated with ASD [43]. Both DPP6 and DPP10 are A-type Kv4 subunits. DPP6 has been shown to be responsible for enhanced A-type K^+ currents in adult hippocampal CA1 pyramidal neuron dendrites [44], thus, mis-expression of *DPP10* may account for the decrease in A-type K^+ currents we observed in this study. Interestingly, most of these 22 overlapping genes (20/22 genes) have been identified as *de novo* variants or CNVs, supporting the increasing observation of *de novo* mutations and CNVs in patients with idiopathic ASD [5, 45–47], and underscoring the importance of developing cellular models that retain the unique genetic features of patients with idiopathic ASD. In addition, in a recent transcriptome analysis of post-mortem autistic brains, researchers identified 444 differentially expressed genes in ASD cortex tissues ($n = 29$) when comparing to control cortex tissues ($n = 29$) [48]. There is a significant ($p\text{-value} = 8{\cdot}12\times10^{-9}$) overlap of 18 genes between 161 differentially expressed genes in autistic patient iPSC-derived neurons and 444 differentially expressed genes in ASD cortex post-mortem tissues (Supplementary Fig. 10). Furthermore, while the remainder of differentially expressed genes have not been previously implicated in ASD, many belong to pathways that have been strongly linked to ASD pathogenesis. For example, GABAergic dysfunction has been repeatedly implicated in ASD with the GABA receptor *GABRB3* perhaps the most significantly associated GABA-related

gene [49], yet we also observed significant mis-expression of other GABA receptors such as *GABRB1*, *GABRA2*, *GABRQ*, and *GABRG2*. Moreover, based on the top-rated gene networks, IPA predicted several upstream or fundamental regulators for our 161 genes, such as *CTNNB1* and *GABRA1. CTNNB1*, also known as β-catenin, have recently been identified as one of the top *de novo* ASD risk contributing mutations [46]. *GABRA1* encodes the α1 subunit of GABA-A receptor. As discussed above, several subunits of GABA-A receptor have been linked to ASD, such as *GABRA4*, *GABRB1*, *GABRB3* [49], indicating the importance role of GABA-A receptor family. *These gene expression results suggest that iPSCs-derived neurons from idiopathic forms of ASD patients maintain the functional genomic properties of idiopathic ASD neural tissue with a fidelity that makes them a great in vitro model.*

Additionally, our assessment of molecular pathways and genetic interaction networks among the differentially expressed genes lends further support that iPSC-neurons derived from idiopathic forms of ASD patients recapitulate the cellular and molecular phenotypes previously associated with ASD. We discovered that the identified differentially expressed genes were highly enriched for pathways related to synaptic structure/activity and ion channels function, which is particularly intriguing given that we identified aberrant voltage-gated ion channel currents in the electrophysiology studies. This additional level of support is particularly important in the context of idiopathic forms of ASD, as there is increasing evidence that the hundreds of genes identified thus far in ASD may ultimately relate to a few signaling networks and/or molecular pathways that underlie the broad ASD phenotype [48, 50].

Finally, gene-disorder association analysis (Autworks) indicated that differentially expressed genes identified in the autistic patient iPSC-neurons were significantly associated not just with ASD, but also with childhood schizophrenia, epilepsy, ADHD and bipolar disorder. These results are in agreement with the well-known overlap of ASD candidate genes with genes previously implicated in these other neurodevelopmental disorders [7], and the blurring diagnostic and genetic boundaries among the common neurodevelopmental disorders [51].

In summary, we demonstrate here that iPSC-derived neurons generated from patients with ASD as compared to unaffected siblings have aberrant cellular and molecular phenotypes that recapitulate previous iPSC studies of syndromic ASD and single gene animal models, and relate to known genetic risk factors for ASD. To further uncover the underlying molecular and cellular basis of idiopathic forms of ASD, approaches such as iPSC-derived neurons will be an important method to obtain tissue for study that appropriately recapitulates the complex dynamics of an autistic patient neural cell. Our results suggest such an approach is feasible and will provide unique insight into cellular and molecular underpinnings of ASD, especially when coupled with robust clinical and phenotypic patient data.

Supplementary Material

Refer to Web version on PubMed Central for supplementary material.

Acknowledgments

We thank Drs. Guibin Chen and Chuangfeng Wu (NHLBI, NIH) for assisting iPSC derivation; Drs. Ren-He Xu and Xue-Jun Li (Univ. of Connecticut Stem Cell Core) for advice and support on hESC line CT-2 and neuronal generation from iPSC; Dr. James Russell, Dr. Vincent Schram and Ms. Holtzclaw Lynne (Microscope Imaging core, NICHD, NIH), and Dr. Lin Lin (NICHD, NIH) for assisting confocal microscopy of synaptic structure; Mr. Chun-Shui Luk (The Chinese Univ. of HK) for assisting microarray analysis. In addition, we extend our gratitude to the children and their families who volunteered their time and efforts during this research.

Funding

This research was supported by the Intramural Research Program of the *Eunice Kennedy Shriver* NICHD at the NIH.

Abbreviations

A-type Kv	Fast inactivating voltage-gated potassium channel
ADHD	Attention deficit hyperactivity disorder
ADI-R	Autism diagnostic interview-revised
ADOS-G	Autism diagnostic observation schedule-generic
ASD	Autism spectrum disorder
bFGF	Basic fibroblast growth factor
cAMP	Cyclic adenosine monophosphate
CGH	Comparative genomic hybridization
CNV	Copy number variation
DAPI	4′,6-diamidino-2-phenylindole
DAVID	Database for Annotation, Visualization and Integrated Discovery
D-type Kv	Slow inactivating voltage-gated potassium channel
FBS	Fetal bovine serum
FDR	False discovery rate
GO	Gene ontology
GWAS	Genome-wide association study
hESC	Human embryonic stem cell
IPA	Ingenuity pathway analysis
iPSC	Induced pluripotent stem cell
MEFs	Mouse embryonic fibroblasts
MRI	Magnetic resonance imaging

NEAA	Non-essential amino acids
NPC	Neural progenitor cell
PBS	Phosphate buffered saline
PCA	Principal component analysis
PSD-95	Post-synaptic density protein 95, now known as DLG4
sEPSC	Spontaneous excitatory postsynaptic current
SFARI	Simons foundation autism research initiative
sIPSC	Spontaneous inhibitory postsynaptic current
SYN	Synaptophysin
TTX	Tetrodotoxin
Tuj1	Tubulin, beta 3 class III or TUBB3
VGAT	Vesicular GABA transporter, now known as SLC32A1
VGLUT1	Vesicular glutamate transporter 1, now known as SLC17A7

References

1. Centers for Disease Control and Prevention. Morbidity and Mortality Weekly Report: Surveillance Summaries. Prevalence of Autism Spectrum Disorder Among Children Aged 8 Years - Autism and Developmental Disabilities Monitoring Network, 11 Sites, United States. 2010
2. Fifth Edition of the Diagnostic and Statistical Manual of Mental Disorders. American Psychiatric Association; 2013. http://www.dsm5.org/Pages/Default.aspx
3. Kim YS, Fombonne E, Koh YJ, Kim SJ, Cheon KA, Leventhal BL. A comparison of DSM-IV pervasive developmental disorder and DSM-5 autism spectrum disorder prevalence in an epidemiologic sample. J Am Acad Child Adolesc Psychiatry. 2014; 53(5):500–8. [PubMed: 24745950]
4. Weiss LA, Arking DE, Daly MJ, Chakravarti A. Gene Discovery Project of Johns H the Autism C. A genome-wide linkage and association scan reveals novel loci for autism. Nature. 2009; 461(7265):802–8. [PubMed: 19812673]
5. Michaelson JJ, Shi Y, Gujral M, Zheng H, Malhotra D, Jin X, et al. Whole-genome sequencing in autism identifies hot spots for de novo germline mutation. Cell. 2012; 151(7):1431–42. [PubMed: 23260136]
6. Pinto D, Pagnamenta AT, Klei L, Anney R, Merico D, Regan R, et al. Functional impact of global rare copy number variation in autism spectrum disorders. Nature. 2010; 466(7304):368–72. [PubMed: 20531469]
7. Betancur C. Etiological heterogeneity in autism spectrum disorders: more than 100 genetic and genomic disorders and still counting. Brain Res. 2011; 1380:42–77. [PubMed: 21129364]
8. SFARI Gene Database. Simons Foundation Autism Research Initiative; 2014. https://gene.sfari.org
9. Bolte S, Willfors C, Berggren S, Norberg J, Poltrago L, Mevel K, et al. The Roots of Autism and ADHD Twin Study in Sweden (RATSS). Twin Res Hum Genet. 2014; 17(3):164–76. [PubMed: 24735654]
10. Kennedy DP, Courchesne E. Functional abnormalities of the default network during self- and other-reflection in autism. Soc Cogn Affect Neurosci. 2008; 3(2):177–90. [PubMed: 19015108]

11. Monk CS, Peltier SJ, Wiggins JL, Weng SJ, Carrasco M, Risi S, et al. Abnormalities of intrinsic functional connectivity in autism spectrum disorders. NeuroImage. 2009; 47(2):764–72. [PubMed: 19409498]
12. Penzes P, Cahill ME, Jones KA, VanLeeuwen JE, Woolfrey KM. Dendritic spine pathology in neuropsychiatric disorders. Nat Neurosci. 2011; 14(3):285–93. [PubMed: 21346746]
13. Takahashi K, Tanabe K, Ohnuki M, Narita M, Ichisaka T, Tomoda K, et al. Induction of pluripotent stem cells from adult human fibroblasts by defined factors. Cell. 2007; 131(5):861–72. [PubMed: 18035408]
14. Brennand KJ, Gage FH. Modeling psychiatric disorders through reprogramming. Dis Model Mech. 2012; 5(1):26–32. [PubMed: 21954066]
15. Lord C, Risi S, Lambrecht L, Cook EH Jr, Leventhal BL, DiLavore PC, et al. The autism diagnostic observation schedule-generic: a standard measure of social and communication deficits associated with the spectrum of autism. J Autism Dev Disord. 2000; 30(3):205–23. [PubMed: 11055457]
16. Lord C, Rutter M, Le Couteur A. Autism Diagnostic Interview-Revised: a revised version of a diagnostic interview for caregivers of individuals with possible pervasive developmental disorders. J Autism Dev Disord. 1994; 24(5):659–85. [PubMed: 7814313]
17. Cheung HH, Liu X, Canterel-Thouennon L, Li L, Edmonson C, Rennert OM. Telomerase protects werner syndrome lineage-specific stem cells from premature aging. Stem cell reports. 2014; 2(4): 534–46. [PubMed: 24749076]
18. Marchetto MC, Carromeu C, Acab A, Yu D, Yeo GW, Mu Y, et al. A model for neural development and treatment of Rett syndrome using human induced pluripotent stem cells. Cell. 2010; 143(4): 527–39. [PubMed: 21074045]
19. Somers A, Jean JC, Sommer CA, Omari A, Ford CC, Mills JA, et al. Generation of transgene-free lung disease-specific human induced pluripotent stem cells using a single excisable lentiviral stem cell cassette. Stem cells. 2010; 28(10):1728–40. [PubMed: 20715179]
20. Zhang SC, Wernig M, Duncan ID, Brustle O, Thomson JA. In vitro differentiation of transplantable neural precursors from human embryonic stem cells. Nat Biotechnol. 2001; 19(12):1129–33. [PubMed: 11731781]
21. Kim JE, O'Sullivan ML, Sanchez CA, Hwang M, Israel MA, Brennand K, et al. Investigating synapse formation and function using human pluripotent stem cell-derived neurons. Proc Natl Acad Sci USA. 2011; 108(7):3005–10. [PubMed: 21278334]
22. Mariani J, Simonini MV, Palejev D, Tomasini L, Coppola G, Szekely AM, et al. Modeling human cortical development in vitro using induced pluripotent stem cells. Proc Natl Acad Sci USA. 2012; 109(31):12770–5. [PubMed: 22761314]
23. Boisvert EM, Denton K, Lei L, Li XJ. The specification of telencephalic glutamatergic neurons from human pluripotent stem cells. J Vis Exp. 2013; 74(74):e50321.
24. Wen Z, Nguyen HN, Guo Z, Lalli MA, Wang X, Su Y, et al. Synaptic dysregulation in a human iPS cell model of mental disorders. Nature. 2014; 515(7527):414–8. [PubMed: 25132547]
25. Cross-Disorder Group of the Psychiatric Genomics Consortium. Identification of risk loci with shared effects on five major psychiatric disorders: a genome-wide analysis. Lancet. 2013; 381(9875):1371–9. [PubMed: 23453885]
26. Nelson TH, Jung JY, Deluca TF, Hinebaugh BK, St Gabriel KC, Wall DP. Autworks: a cross-disease network biology application for Autism and related disorders. BMC Med Genomics. 2012; 5:56. [PubMed: 23190929]
27. Courchesne E, Pierce K, Schumann CM, Redcay E, Buckwalter JA, Kennedy DP, et al. Mapping early brain development in autism. Neuron. 2007; 56(2):399–413. [PubMed: 17964254]
28. Stoner R, Chow ML, Boyle MP, Sunkin SM, Mouton PR, Roy S, et al. Patches of disorganization in the neocortex of children with autism. N Engl J Med. 2014; 370(13):1209–19. [PubMed: 24670167]
29. Courchesne E, Pierce K. Why the frontal cortex in autism might be talking only to itself: local over-connectivity but long-distance disconnection. Curr Opin Neurobiol. 2005; 15(2):225–30. [PubMed: 15831407]

30. Spooren W, Lindemann L, Ghosh A, Santarelli L. Synapse dysfunction in autism: a molecular medicine approach to drug discovery in neurodevelopmental disorders. Trends Pharmacol Sci. 2012; 33(12):669–84. [PubMed: 23084458]

31. Kenny EM, Cormican P, Furlong S, Heron E, Kenny G, Fahey C, et al. Excess of rare novel loss-of-function variants in synaptic genes in schizophrenia and autism spectrum disorders. Mol Psychiatry. 2014; 19(8):872–9. [PubMed: 24126926]

32. Ananiev G, Williams EC, Li H, Chang Q. Isogenic pairs of wild type and mutant induced pluripotent stem cell (iPSC) lines from Rett syndrome patients as in vitro disease model. PloS one. 2011; 6(9):e25255. [PubMed: 21966470]

33. Cheung AY, Horvath LM, Grafodatskaya D, Pasceri P, Weksberg R, Hotta A, et al. Isolation of MECP2-null Rett Syndrome patient hiPS cells and isogenic controls through X-chromosome inactivation. Hum Mol Genet. 2011; 20(11):2103–15. [PubMed: 21372149]

34. Paşca SP, Portmann T, Voineagu I, Yazawa M, Shcheglovitov A, Pasca AM, et al. Using iPSC-derived neurons to uncover cellular phenotypes associated with Timothy syndrome. Nat Med. 2011; 17(12):1657–62. [PubMed: 22120178]

35. Yang J, Cai J, Zhang Y, Wang X, Li W, Xu J, et al. Induced pluripotent stem cells can be used to model the genomic imprinting disorder Prader-Willi syndrome. J Biol Chem. 2010; 285(51): 40303–11. [PubMed: 20956530]

36. Shcheglovitov A, Shcheglovitova O, Yazawa M, Portmann T, Shu R, Sebastiano V, et al. SHANK3 and IGF1 restore synaptic deficits in neurons from 22q13 deletion syndrome patients. Nature. 2013; 503(7475):267–71. [PubMed: 24132240]

37. Germain ND, Chen PF, Plocik AM, Glatt-Deeley H, Brown J, Fink JJ, et al. Gene expression analysis of human induced pluripotent stem cell-derived neurons carrying copy number variants of chromosome 15q11-q13·1. Mol Autism. 2014; 5:44. [PubMed: 25694803]

38. Griesi-Oliveira K, Acab A, Gupta AR, Sunaga DY, Chailangkarn T, Nicol X, et al. Modeling non-syndromic autism and the impact of TRPC6 disruption in human neurons. Mol Psychiatry. 2014; 20(11):1350–1365. [PubMed: 25385366]

39. Bauman ML, Kemper TL, Arin DM. Pervasive neuroanatomic abnormalities of the brain in three cases of Rett's syndrome. Neurology. 1995; 45(8):1581–6. [PubMed: 7644058]

40. Chen RZ, Akbarian S, Tudor M, Jaenisch R. Deficiency of methyl-CpG binding protein-2 in CNS neurons results in a Rett-like phenotype in mice. Nat Genet. 2001; 27(3):327–31. [PubMed: 11242118]

41. Eijkelkamp N, Linley JE, Baker MD, Minett MS, Cregg R, Werdehausen R, et al. Neurological perspectives on voltage-gated sodium channels. Brain. 2012; 135(9):2585–2612. [PubMed: 22961543]

42. Schmunk G, Gargus JJ. Channelopathy pathogenesis in autism spectrum disorders. Frontiers in genetics. 2013; 4:222.doi: 10.3389/fgene.2013.00222 [PubMed: 24204377]

43. Guglielmi L, Servettini I, Caramia M, Catacuzzeno L, Franciolini F, D'Adamo MC, et al. Update on the implication of potassium channels in autism: K(+) channelautism spectrum disorder. Frontiers in cellular neuroscience. 2015; 9:34. [PubMed: 25784856]

44. Sun W, Maffie JK, Lin L, Petralia RS, Rudy B, Hoffman DA. DPP6 establishes the A-type K(+) current gradient critical for the regulation of dendritic excitability in CA1 hippocampal neurons. Neuron. 2011; 71(6):1102–15. [PubMed: 21943606]

45. Neale BM, Kou Y, Liu L, Ma'ayan A, Samocha KE, Sabo A, et al. Patterns and rates of exonic de novo mutations in autism spectrum disorders. Nature. 2012; 485(7397):242–5. [PubMed: 22495311]

46. O'Roak BJ, Vives L, Girirajan S, Karakoc E, Krumm N, Coe BP, et al. Sporadic autism exomes reveal a highly interconnected protein network of de novo mutations. Nature. 2012; 485(7397): 246–50. [PubMed: 22495309]

47. Ronemus M, Iossifov I, Levy D, Wigler M. The role of de novo mutations in the genetics of autism spectrum disorders. Nat Rev Genet. 2014; 15(2):133–41. [PubMed: 24430941]

48. Voineagu I, Wang X, Johnston P, Lowe JK, Tian Y, Horvath S, et al. Transcriptomic analysis of autistic patient brain reveals convergent molecular pathology. Nature. 2011; 474(7351):380–4. [PubMed: 21614001]

49. Coghlan S, Horder J, Inkster B, Mendez MA, Murphy DG, Nutt DJ. GABA system dysfunction in autism and related disorders: from synapse to symptoms. Neurosci Biobehav Rev. 2012; 36(9): 2044–55. [PubMed: 22841562]

50. Ghosh A, Michalon A, Lindemann L, Fontoura P, Santarelli L. Drug discovery for autism spectrum disorder: challenges and opportunities. Nat Rev Drug Discov. 2013; 12(10):777–90. [PubMed: 24080699]

51. Carroll LS, Owen MJ. Genetic overlap between autism, schizophrenia and bipolar disorder. Genome Med. 2009; 1(10):102. [PubMed: 19886976]

52. Shaffer D, Gould MS, Brasic J, Ambrosini P, Fisher P, Bird H, et al. A children's global assessment scale (CGAS). Arch Gen Psychiatry. 1983; 40(11):1228–31. [PubMed: 6639293]

53. Wagner A, Lecavalier L, Arnold LE, Aman MG, Scahill L, Stigler KA, et al. Developmental disabilities modification of the Children's Global Assessment Scale. Biol Psychiatry. 2007; 61(4): 504–11. [PubMed: 17276748]

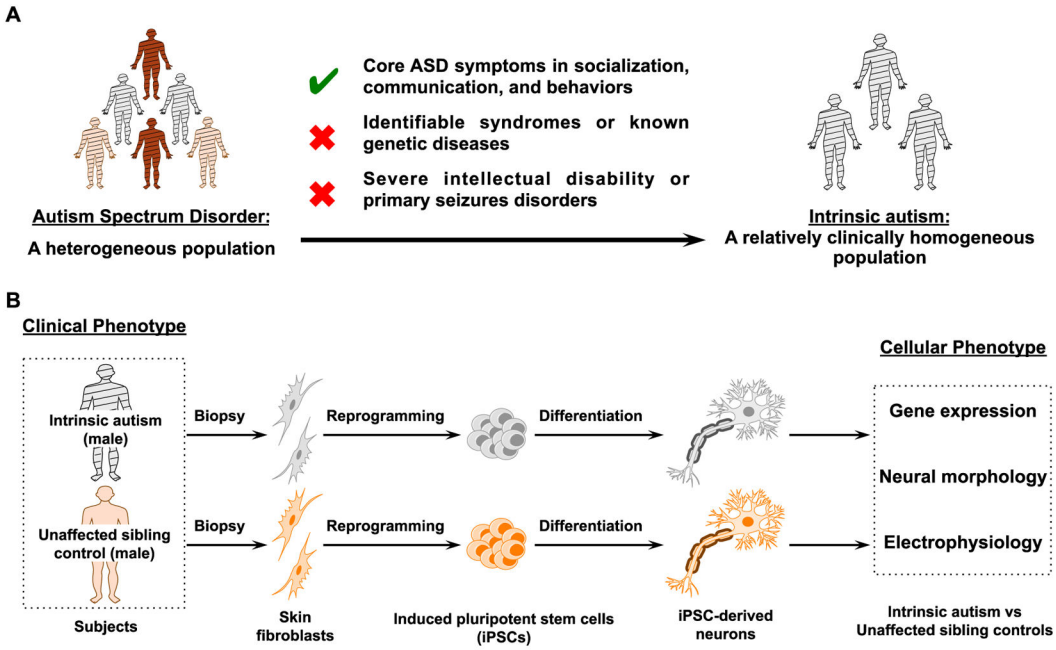

Figure 1. Experimental scheme of applying iPSC methodology for development of a cellular model in a clinically homogeneous subset of patients with ASD

(A) We studied a clinically homogeneous patient population of boys with idiopathic forms of ASD ("intrinsic autism") by excluding patients with known genetic disease or recognizable syndromes, as well as exclusion of those with severe intellectual disability or primary seizure disorders. **(B)** To assess the neural cellular and molecular phenotypes of ASD, we created iPSCs from skin fibroblasts from autistic boys and their unaffected male siblings and then differentiated these iPSCs into electrophysiologically active neurons. Assays for gene expression, neurite outgrowth, synaptic density, and electrophysiology were used to compare autistic patient and control iPSC-derived neurons.

See also Table 1, Supplementary Table 2 for patient and cell line information.

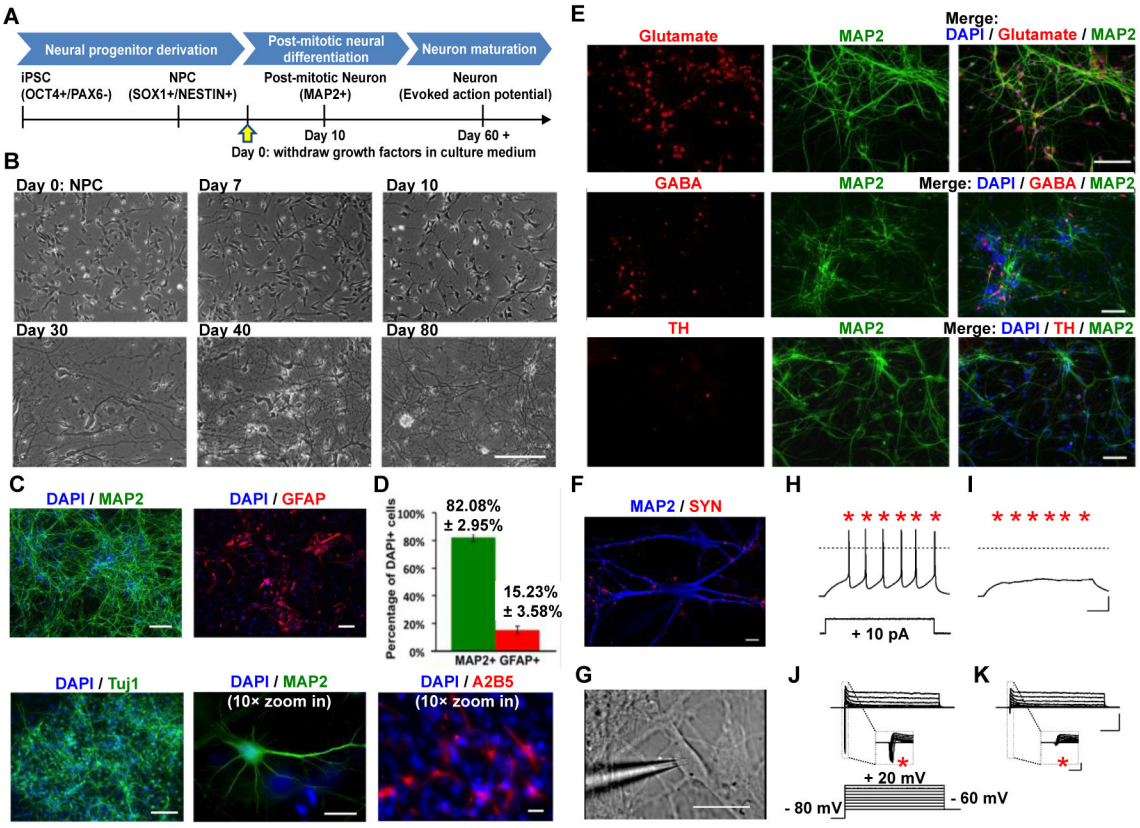

Figure 2. Derivation of neurons from patient-specific iPSCs

(A) Schematic timeline for neural differentiation protocol from iPSCs through NPC intermediate. **(B)** Sample bright-field images depicting morphological changes during neurons differentiation from NPCs. Bar = 200 μm. **(C)** Immunocytochemistry for the neuronal markers MAP2 or Tuj1 (green) indicates the presence of post-mitotic neurons in 80-day-old iPSC-derived monolayer neuronal cultures. GFAP- or A2B5-positive astrocytes (red) are also present after 80 days of neural differentiation. Bar = 100 μm, except Bar in 10× zoom in pictures represents 20 μm. **(D)** 82% MAP2-positive neurons and 15% GFAP-positive astrocytes were observed in our cultures with this protocol, as measured by MAP2-positive cells and GFAP-positive cells over total cell number as visualized by DAPI staining. The bars show mean ± S.D.. **(E)** Assessment of neural subtypes of iPSC-derived neurons. A majority population of MAP2-positive neurons (70%) expressed glutamate, around 30% of neurons expressed GABA, and less than 5% expressed TH. Bar = 100 μm. **(F)** Sample confocal image of immunostaining for SYP (red) and MAP2 (blue) of iPSC-derived neurons at 80 days after neuronal differentiation. Bar = 10 μm. **(G–K)** Electrophysiological properties of 80-days-old iPSC-derived neurons. **(G)** Sample differential interference contrast infrared image showing morphology of iPSC-derived neuron patched for electrophysiological recording. Bar = 50 μm. **(H)** Representative recordings of voltage traces showing evoked action potentials (evoked by +10 pA current step, 1s). **(I)** Bath application of the selective Na^+ channel antagonist TTX (1 μM) suppressed evoked AP (bars = 20 mV, 200 ms). **(J)** Representative recordings of current traces showing inward voltage gated Na^+ current and outward voltage gated K^+ currents in response to depolarization (from −60 mV

to +20 mV, ΔV = 10 mV, V_{hold} = −80 mV, 500 ms). **(K)** Bath application of the selective Na^+ channel antagonist TTX (1 μM) abolished fast inward currents (bars = 1 nA, 10 ms; insert bars = 1 nA, 10 ms). SYN = Synaptophysin; TH = Tyrosine hydroxylase; TTX = Tetrodotoxin.

See also Supplementary Fig. 1–6 for generation, characterization of iPSC and NPC.

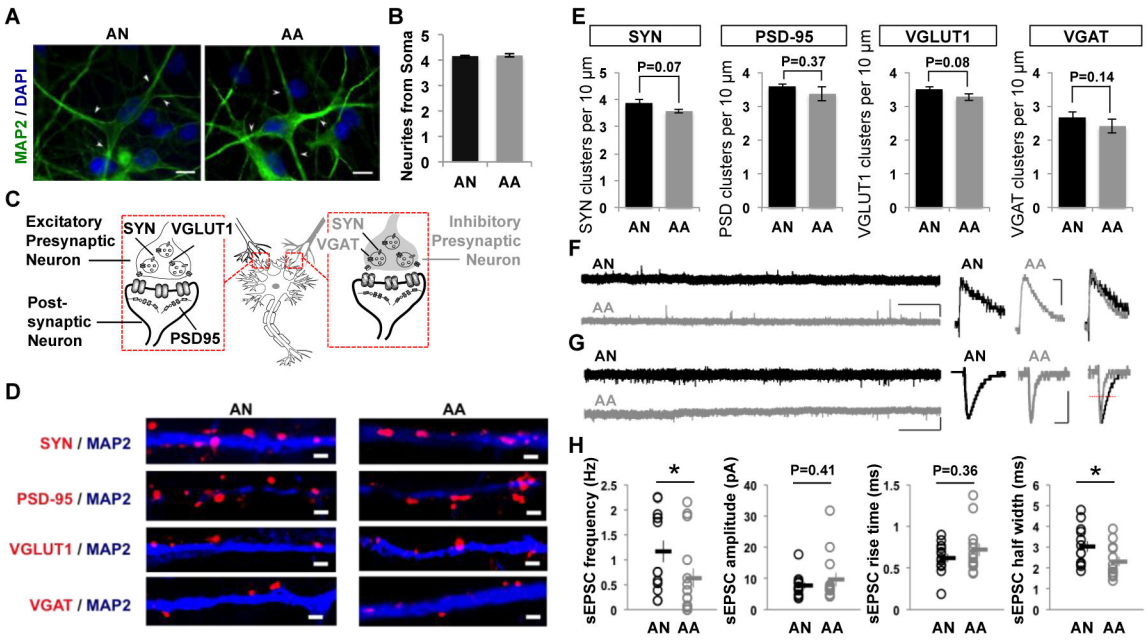

Figure 3. Neurons derived from autistic patient (AA) iPSCs displayed altered spontaneous synaptic activities when compared to unaffected male sib control (AN) iPSC-derived neurons

(A–B) Neurites number unaltered between AA and AN iPSC-derived neurons. **(A)** Neurites and soma body of neurons were immunolabelled with MAP2 antibody (green) and nuclei were visualized by DAPI staining (blue). Neurites indicated by white arrow. Bar = 10 µm. **(B)** Quantification of neurites numbers showing no significant difference between AA and AN neurons. Values represent mean ± SEM. n = 200 neurons. **(C–E)** Synaptic density unaltered between AA and AN neurons. **(C)** Schematic of synaptic localization of synaptic proteins. **(D)** Neurons were immunostained with MAP2 antibody (blue) to highlight the dendritic arbor, and synaptic protein antibodies (red): SYN to visualize presynaptic boutons, or PSD-95 to visualize postsynaptic sites, or VGLUT1, or VGAT. Bar = 2 µm. **(E)** Summaries of quantification of synaptic protein cluster number per 10 µm dendrite length for SYN, PSD-95, VGLUT1 and VGAT for AN neurons (n = 26, 28, 28, 24) and AA neurons (n = 24, 29, 30, 25). Values represent mean ± SEM. **(F)** Spontaneous inhibitory post-synaptic current (sIPSC) in iPSC-derived neurons. Sample traces of sIPSCs (bars = 20 pA, 10 s) and average sIPSC (bars = 10 pA, 10 ms) recorded in AN (black) or AA (gray) neurons. **(G)** Spontaneous excitatory post-synaptic current (sEPSC) in iPSC-derived neurons. Sample traces of sEPSCs (bars = 20 pA, 10 s) and average sEPSC (bars = 5 pA, 5 ms) recorded in AN (black) or AA (gray) neurons. **(H)** Summary of quantification for pooled data values of sEPSC frequency (AN: n = 13, AA: n = 15), amplitude, rise time and half width (AN: n =13, AA: n =13). * $p < 0{\cdot}05$. sEPSC = Spontaneous excitatory postsynaptic current; sIPSC = Spontaneous inhibitory postsynaptic current.

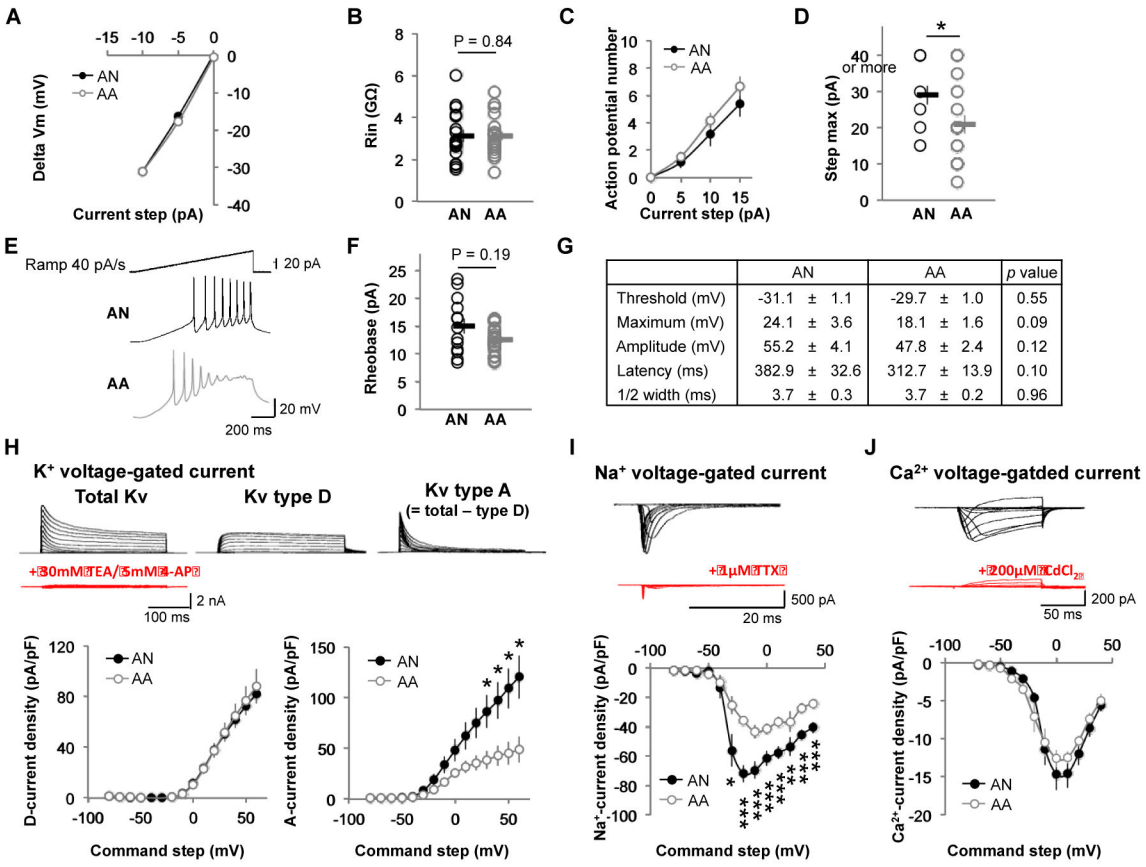

	AN	AA	*p* value
Threshold (mV)	-31.1 ± 1.1	-29.7 ± 1.0	0.55
Maximum (mV)	24.1 ± 3.6	18.1 ± 1.6	0.09
Amplitude (mV)	55.2 ± 4.1	47.8 ± 2.4	0.12
Latency (ms)	382.9 ± 32.6	312.7 ± 13.9	0.10
1/2 width (ms)	3.7 ± 0.3	3.7 ± 0.2	0.96

Figure 4. Comparison of intrinsic electrophysiological properties of iPSC-derived neurons between AA and AN

(A) The amplitudes of the steady state membrane potentials are plotted against injected negative current steps (AN: $n = 17$, AA: $n = 20$). **(B)** Group data showing no difference in input resistance between AA and AN neurons (AN: $n = 17$, AA: $n = 20$). **(C)** Graph showing the number of action potentials (APs) evoked for a range of positive current injections (AN: $n = 16$, AA: $n = 20$). **(D)** Group data showing the decrease of the maximal current step (before APs saturation) in AA neurons (AN: $n = 15$, AA: $n = 17$). * $p < 0{\cdot}05$. **(E)** The Representative voltage traces evoked by a current ramp of 40 pA/s from AN (black) and AA (gray) neurons (bars = 20 pA, 20 mV, 200 ms). **(F)** The rheobase is not different between AN (black) and AA (gray) neurons (AN: $n = 13$, AA: $n = 20$). **(G)** Parameters of the first AP evoked by a current ramp 40 pA/s (AN: $n = 13$, AA: $n = 20$). **(H–J)** Voltage-gated currents in iPSC-derived neurons. **(H)** K^+ voltage-gated current. Top, family of total Kv currents (left; evoked by voltage command from −80 mV to +60 mV and V_{hold} = −80 mV), family of slow Kv currents (Kv type D) (middle; evoked by voltage command from −80 mV to +60 mV and V_{hold} = −30 mV). The fast Kv current (Kv type A, right) is isolated by subtracting these two Kv currents (type A = total – type D) (bars = 2 nA, 100 ms). Bath application of 30 mM TEA and 5 mM 4-AP (red), non-selective K^+ channel blockers, suppressed Kv currents. Bottom, I/V plots of Kv type D (left) and type A (right) from AN (black) and AA (gray) neurons (AN: $n = 6$, AA: $n = 6$). * $p < 0{\cdot}05$. **(I)** Na^+ voltage-gated current. Top, family of Na^+ currents evoked by voltage command from −80 to +40 mV and V_{hold} = −80

mV (bars = 500 pA, 20 ms). Bath application of the selective Na^+ channel antagonist TTX (1 μM) suppressed Na^+ current (red). Bottom, I/V curve showing a reduction of Na^+ current in AA (gray) neurons compared to AN (black) (AN: $n = 9$, AA: $n = 11$). * $p < 0{\cdot}05$. ** $p < 0{\cdot}01$. *** $p < 0{\cdot}005$. **(J)** Ca^{2+} voltage-gated current. Top, family of Ca^{2+} currents evoked by voltage command from −70 to +40 mV and $V_{hold} = -80$ mV (bars = 200 pA, 50 ms). Bath application of 200 μM $CdCl_2$ (red), a non-selective Ca^{2+} channel blocker, suppressed Ca^{2+} currents. Bottom, I/V curve of Ca^{2+} current from AN (black) and AA (gray) neurons (AN: $n = 12$, AA: $n = 9$). 4-AP = 4-aminopyridine; TEA = Tetraethylammonium; TTX = Tetrodotoxin.

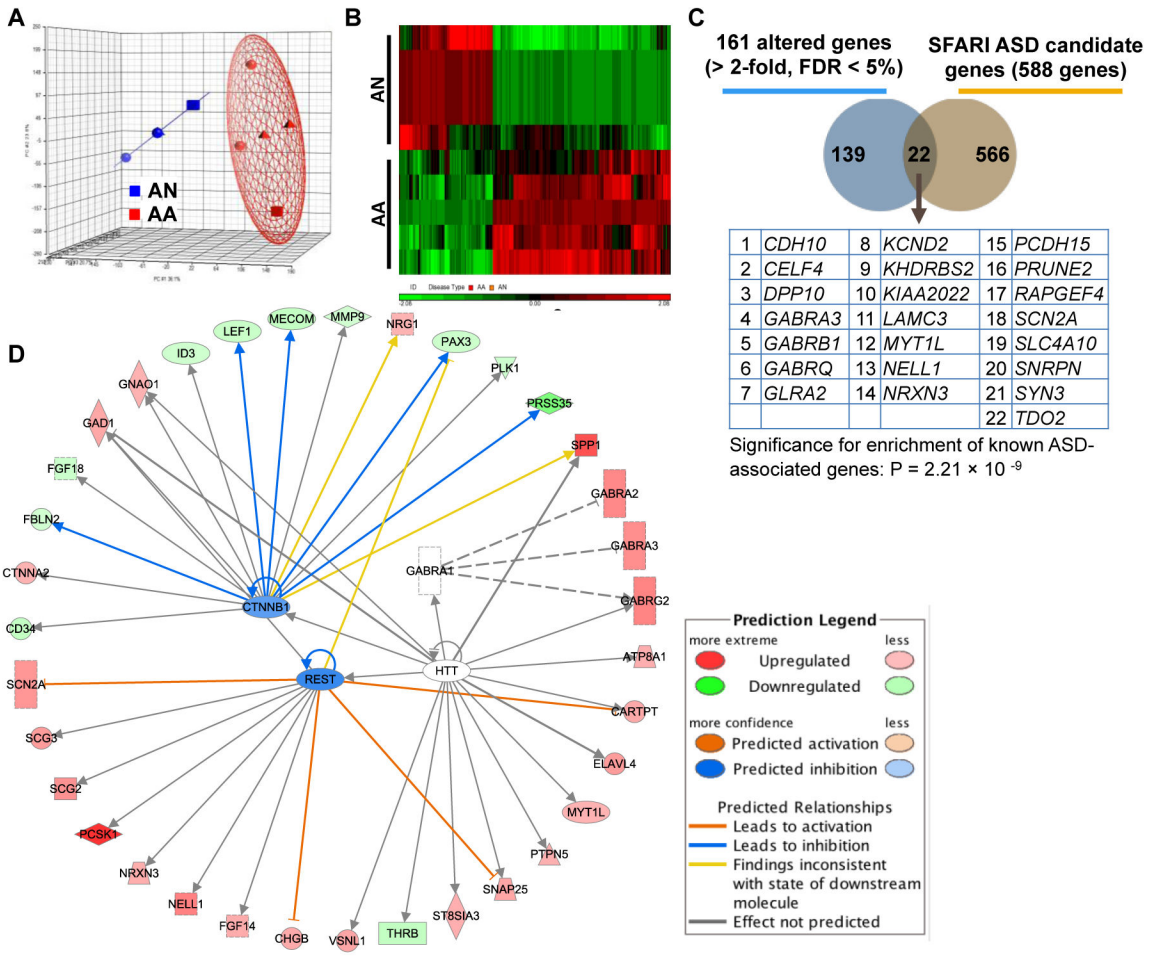

Figure 5. Genome-wide microarray gene analysis of iPSC-derived neurons from AA and AN

(A) PCA Mapping of microarray gene expression profile for iPSC-derived neurons from AA (red) and AN (blue). **(B)** Heat map showing 161 differentially expressed genes with greater than two-fold changes in AA neurons as compared to AN neurons at FDR < 5%. Green color refers to low levels of gene expression and red color to high level of gene expression. **(C)** Venn diagram illustrating the overlapping of 22 genes between 161 differentially expressed genes from autistic neurons and 588 ASD candidate genes from previous published studies (SFARI database, 2014). Table showing the list of 22 overlapping genes and this enrichment for known ASD-associated genes was highly significant (*p-value* = 2·21 × 10^{-9}, calculated by hypergeometric probability test). **(D)** Predicted upstream regulators and networks for 161 differentially expressed genes in autistic patient iPSC-derived neurons generated by IPA. IPA analysis predicted the upstream regulators and networks for 161-gene set, such as *REST*, *CTNNB1*, *HTT*, and *GABRA1*. CTNNB1 = catenin (cadherin-associated protein), β1; HTT = Huntingtin, a disease gene linked to a neurodegenerative disorder Huntington's disease; GABRA1 = α1 subunit of GABA-A receptor; FDR = False discovery rate; IPA = Ingenuity pathway analysis; PCA = Principal component analysis; REST = RE1 silencing transcription factor; SFARI = Simons foundation autism research initiative.

See also Supplementary Fig. 10 and Supplementary Tables 2–4 for gene list, more bioinformatics analysis.

Table 1

Summary of clinical features for the participants [a]

Trait	Participants number					
	AA1	**AN1 (Sib of AA1)**	**AA2**	**AN2 (Sib of AA2)**	**AA3**	**AN3 (Sib of AA3)**
General Information						
Sex/Age at testing (years)	M/8	M/10	M/7	M/16	M/9	M/7
Ethnicity	Caucasians	Caucasians	Caucasians	Caucasians	Asian-Indian	Asian-Indian
Primary Diagnosis						
Autism Spectrum Disorder	+	−	+	−	+	−
ADOS-G score[b]	8		8		9	
Family History						
Family member with neurologic diseases, Mental retardation, intellectual disability, ADHD, speech disorders	Half uncle with intellectual disability (etiology unknown)		Normal on examination		Paternal cousin with speech delay (etiology unknown); Paternal uncle with learning disability (etiology unknown)	
Parental, pregnancy and birth History						
Parental Age (Father / Mother) (years)	34/26	32/24	35/37	25/27	29/24	31/26
Maternal fever, Infection, Medication; Cesarean section, Length/weight for gestational age	Normal on examination					
Birth length (cm)/weight (kg)	49·53 / 3·63		*N/A* / 3·58		*N/A* / 3·71	
Physical features						
Frontal-occipital circumference (cm)	54·3		52·0		53·2	
Dysmorphism, Macrocephaly, Microcephaly, Eczema, Cleft palate, Short stature	Normal on examination					
Developmental History						

Trait	Participants number					
	AA1	**AN1 (Sib of AA1)**	**AA2**	**AN2 (Sib of AA2)**	**AA3**	**AN3 (Sib of AA3)**
Age (months) start sitting / walking	6 / 10		*N/A* / 12		*N/A* / 12	
Poor feeding, sitting, walking as infant	Normal on examination					
Age (months) start single words/phrases	48 / *N/A*		18 / 24		30 / 34	
Language delay	Moderate to Severe	Normal	Moderate	Normal	Moderate	Normal
Cognitive delay	Moderate	Normal	Moderate	Normal	Moderate	Normal
Developmental History						
CGAS score (1 through 100)[c]	*N/A*	90	45	90	45	*N/A*
DD-CGAS score (1 through 100)[d]	*N/A*	90	55	90	49	*N/A*
Intellectual disability	Moderate	Normal	Moderate	Normal	Moderate	Normal
Additional abnormal behaviors						
Anxiety and depression, Aggression (self-injurious), Obsessive-compulsive disorder (OCD), Attention deficit hyperactivity disorder (ADHD)	OCD, ADHD	–	–	–	–	–
Additional Diagnosis						
Severe intellectual disability	–	–	–	–	–	–
Primary seizure disorder	–	–	–	–	–	–
Identifiable syndromes (e.g. Fragile X syndrome)	–	–	–	–	–	–
Identifiable known genetic diseases by clinical and CGH diagnosis	–	–	–	–	–	–
Subjective sleep disturbance	Decreased REM sleep	–	–	–	–	–
EGG abnormality	–	–	–	–	–	–
Hearing impairment	–	–	–	–	–	–

Trait	Participants number					
	AA1	AN1 (Sib of AA1)	AA2	AN2 (Sib of AA2)	AA3	AN3 (Sib of AA3)
CNS abnormality by MRI	–	–	–	–	–	–
Cardiovascular abnormality	–	–	–	–	–	–

[a]Symbol and abbreviation: "+" = Present; "−" = Absent; "N/A" = This clinical data is not available; CGH = Comparative genomic hybridization; REM, rapid eye movement.

[b]ADOS-G (Lord *et al.*, 2000): The Autism Diagnostic Observation Schedule - Generic (ADOS-G) is a semi-structured, standardized assessment tool that can be used with children and adults to determine presence of behaviors that are consistent with a diagnosis of ASD. This tool assesses one's abilities and behaviors in the areas of social interaction, communication, play, and imaginative use of objects. The scoring of a subset of these behaviors are then summed for a one combined score for "Communication and Social Interaction domain", and the cut-off for ASD is 7.

[c]CGAS (Shaffer *et al.*, 1983): The Children's Global Assessment Scale (CGAS) is a measure to provide a global measure of level of functioning in children and adolescents. The measure provides a single global rating only, on scale of 0–100. In making their rating, the clinician makes use of the glossary details to determine the meaning of the points on the scale. CGAS score 50-41 indicates "Moderate impaired functioning in most areas or severe in one area".

[d]DD-CGAS (Wagner *et al.*, 2007): The Developmental Disabilities-Children's Global Assessment Scale (DD-CGAS) was adapted from CGAS for assessing children having ASD. CGAS score 55-49 indicates "Moderate impairment in functioning in most domains and severe impairment in at least one domain (e.g., daily living or communication)".

Table 2

Most significant GO terms, biological functions, and disorders associated with 161 differentially expressed genes in autistic patient iPSC-derived neurons [a]

Gene Ontology Term & Category	Enrichment *p* value
GO term (*GO ID*)	
Biological process	
Nervous system development (*GO: 0007399*)	7·0E-10
Transmission of nerve impulse (*GO: 00192260*)	4·2E-07
Cellular component	
Synapse (*GO: 0045202*)	9·5E-06
Ion channel complex (*GO: 0034702*)	6·0E-05
Extracellular matrix (*GO: 0031012*)	1·6E-04
Integral to plasma membrane (*GO: 0005887*)	3·7E-04
Neuron projection (*GO: 0043005*)	2·4E-03
Molecular function	
Neurotransmitter receptor activity (*GO: 0030594*)	1·6E-05
Neurotransmitter binding (*GO: 0030594*)	2·6E-05
Gated channel activity (*GO: 0022836*)	6·4E-05
Ion channel activity (*GO: 0005216*)	4·3E-04
KEGG pathway (*pathway ID*)	
Nicotine addiction (*hsa05033*)	8·4E-07
GABAergic synapse (*hsa04727*)	8·3E-06
Morphine addiction (*hsa05032*)	8·9E-06
Retrograde endocannabinoid signaling (*hsa04723*)	2·0E-05
Neuroactive ligand-receptor interaction (*hsa04080*)	6·6E-05
PI3K-Akt signaling pathway (*hsa04151*)	1·9E-03
ECM-receptor interaction (*hsa04512*)	5·8E-03
Panther pathway (*pathway ID*)	
Cadherin signaling pathway (*P00012*)	5·9E-02
Metabotropic glutamate receptor group II pathway (*P00040*)	8·7E-02

Gene Ontology Term & Category	Enrichment *p* value
Ionotropic glutamate receptor pathway (*P00037*)	9·6E-02
Associated disease (Autworks: Gene-disease association analysis)	
Schizophrenia, Childhood	2·0E-03
Waardenburg's Syndrome	4·0E-03
Neurotic Disorders	6·0E-03
Epilepsy, Generalized	6·0E-03
Multiple Sclerosis, Chronic Progressive	4·2E-02
Autistic Disorder	4·9E-02

[a]Source of analysis:

Partek Genomics Suite; DAVID Bio-informational database; Ingenuity Pathway Analysis database; Autworks Gene-disease association analysis.

Abbreviations: Akt = A serine/threonine-specific protein kinase, also known as Protein kinase B; ECM = Extracellular matrix; PI3K = Phosphatidylinositol-4,5-bisphosphate 3-kinase, now known as PIK3CA.

Table 3

Most significant gene interaction networks associated with 161 differentially expressed genes in autistic patient iPSC-derived neurons [a]

Network ID [b]	Number of Genes [c]	Top Diseases and Functions	Score [d]	Major Network-nodes [e]
1	24	Nervous System Development and Function, Tissue Morphology, Hereditary Disorder	47	ERK1/2, Integrin
2	23	Psychological Disorders, Neurological Disease, Nutritional Disease	45	Insulin, GABA-receptors
3	16	Behavior, Neurological Disease, Amino Acid Metabolism	28	ERK, MAPK, MMP9, CREB
4	15	Cell Morphology, Amino Acid Metabolism, Small Molecule Biochemistry	25	Ubiquitin C
5	15	Cell Death and Survival, Cell Cycle, Cellular Compromise	23	TP53, APP, β-estradiol, L-triiodothyronine
6	15	Cell Death and Survival, Tumor Morphology, Carbohydrate Metabolism	23	Akt, PI3K
7	13	Cell Death and Survival, Tumor Morphology, Nervous System Development and Function	21	TGFβ, DNF, STAT3, SHH
8	12	Cellular Development, Cellular Growth and Proliferation, Developmental Disorder	19	Ubiquitin C, PKD1, TERF2
9	10	Cellular Function and Maintenance, Molecular Transport, Carbohydrate Metabolism	15	Ca^{2+}, HTT
10	7	Hereditary Disorder, Neurological Disease, Ophthalmic Disease	9	PI3k complex, MAPK, Caspase

[a] Source of analysis: Ingenuity Pathway Analysis database (IPA)

[b] Network ID: See Supplementary Fig. 7–9 for corresponding network illustrations.

[c] Number of genes: Number of genes from 161 dataset involved in the given network.

[d] Score of IPA network: The score, derived from a *p-value*, is a numerical value used to rank networks according to their degree of relevance to the network eligible molecules in the experiment dataset of genes. Higher score indicates lower probability of finding the observed number of network eligible molecules in a given network by random chance.

[e] Abbreviations: Akt = A serine/threonine-specific protein kinase, also known as Protein kinase B (PKB); APP = Amyloid beta (A4) precursor protein; BDNF = Brain-derived neurotrophic factor; Caspase(s) = Cysteine-aspartic protease(s); CREB = cAMP responsive element binding protein; ERK1/2 = Extracellular signal-regulated kinases 1/2; ERK1 = Mitogen-activated protein kinase 3, now known as MAPK3; ERK2 = Mitogen-activated protein kinase 1, now known as MAPK1; HTT = Huntingtin, a disease gene linked to a neurodegenerative disorder Huntington's disease; MAPK = Mitogen-activated protein kinase; MMP9 = Matrix metallopeptidase 9; PI3K = Phosphatidylinositol-4,5-bisphosphate 3-kinase, now known as PIK3CA; PKD1 = Polycystic kidney disease 1; SHH = Sonic hedgehog; STAT3 = Signal transducer and activator of transcription 3; TERF2 = Telomeric repeat binding factor 2; TGFβ = Transforming growth factor beta; TP53 = Tumor protein p53.